REPORT DOCUMENTATION PAGE

Form Approved
OMB No. 0704-0188

1. REPORT DATE *(DD-MM-YYYY)*	**2. REPORT TYPE**	**3. DATES COVERED** *(From - To)*
07/10/2009	Final	15/02/2006-31/05/2009

4. TITLE AND SUBTITLE
Multi-Scale Modeling for Combined Shock-Shear Initiation of

Energetic Solids

5a. CONTRACT NUMBER
FA9550-06-1-0121

5b. GRANT NUMBER

5c. PROGRAM ELEMENT NUMBER

6. AUTHOR(S)
Keith A. Gonthier

5d. PROJECT NUMBER

5e. TASK NUMBER

5f. WORK UNIT NUMBER

7. PERFORMING ORGANIZATION NAME(S) AND ADDRESS(ES)

Louisiana State University
Mechanical Engineering Dept.
2508 Patrick F. Taylor Hall
Baton Rouge, Louisiana 70803

8. PERFORMING ORGANIZATION REPORT NUMBER

9. SPONSORING / MONITORING AGENCY NAME(S) AND ADDRESS(ES)
AFOSR

10. SPONSOR/MONITOR'S ACRONYM(S)

11. SPONSOR/MONITOR'S REPORT NUMBER(S)

12. DISTRIBUTION / AVAILABILITY STATEMENT A

13. SUPPLEMENTARY NOTES

14. ABSTRACT
Multi-scale interactions between initially planar deformation waves in heterogeneous energetic solids and macro-scale boundaries were computationally examined to characterize wave interaction structures and dissipative heating responsible for combustion initiation. The macro-scale response was described by a continuum theory that accounts for elastic and inelastic volumetric deformation in a thermodynamically consistent manner. The meso-scale response was described by conservation principles and an elastic-viscoplastic constitutive theory to predict contact induced nonlinear deformation and thermomechanical fields within particles. Predicted meso-scale fields were locally averaged and compared to independent predictions given by the macro-scale model. Wave-boundary interactions resulted in dispersed wave structures that are analogous to Mach stems in gas dynamics, with maximum dissipative heating rates occurring along bounding surfaces away from the stagnation region, which substantially increased the fraction of mass locally heated to elevated temperature.

15. SUBJECT TERMS
granular explosive, dynamic compaction, macro-scale modeling, meso-scale modeling, hot-spots

16. SECURITY CLASSIFICATION OF: U			**17. LIMITATION OF ABSTRACT**	**18. NUMBER OF PAGES**	**19a. NAME OF RESPONSIBLE PERSON**
a. REPORT	**b. ABSTRACT**	**c. THIS PAGE**	UU	24	Keith A. Gonthier
					19b. TELEPHONE NUMBER *(include area coc* 225-578-5915

Standard Form 298 (Rev. 8-98)
Prescribed by ANSI Std. Z39.18

Multi-Scale Modeling for Combined Shock-Shear Initiation of Energetic Solids*

Keith A. Gonthier
Associate Professor
Mechanical Engineering Department
Louisiana State University
Baton Rouge, LA 70803, USA
Phone: 225-578-5915
FAX: 225-578-5924
Email: *gonthier@me.lsu.edu*

Abstract

Multi-scale interactions between initially planar deformation waves in heterogeneous energetic solids and macro-scale boundaries were computationally examined to characterize wave interaction structures and dissipative heating responsible for combustion initiation. The macro-scale response was described by a continuum theory that accounts for elastic and inelastic volumetric deformation in a thermodynamically consistent manner; the model equations were numerically integrated in terms of generalized curvilinear coordinates using a high-resolution shock-capturing technique. The meso-scale scale response was described by conservation principles and an elastic-viscoplastic constitutive theory to predict contact induced nonlinear deformation and thermomechanical fields within particles; the model equations were numerically integrated using a combined finite and discrete element technique. Predicted meso-scale fields were locally averaged and compared to independent predictions given by the macro-scale model. Wave-boundary interactions resulted in dispersed wave structures that are analogous to Mach stems in gas dynamics, with maximum dissipative heating rates occurring within the stem region along bounding surfaces away from the stagnation region. These maximum heating rates substantially increased the fraction of mass locally heated to elevated temperature. Bulk shear was shown to have a small effect on dissipative heating for the impact conditions investigated in this study. The dependence of wave structure, dissipative heating rate, and hot-spot mass fraction on initial wave strength was characterized. Macro- and meso-scale predictions agreed well, provided that the averaging volume size was suitably chosen.

1 Significance

Interaction between deformation waves in heterogeneous energetic solids and macro-scale boundaries may trigger prompt vigorous combustion due to locally high dissipative heating rates. For example, Wilson, et al [11], experimentally showed that interaction between an initially planar shock in the explosive PBXW-128 (60% HMX and 40% polymeric binder) and a hemispherical glass anvil

*Final report for AFOSR Contract Number FA9550-06-1-0121. Submitted October 7, 2009.

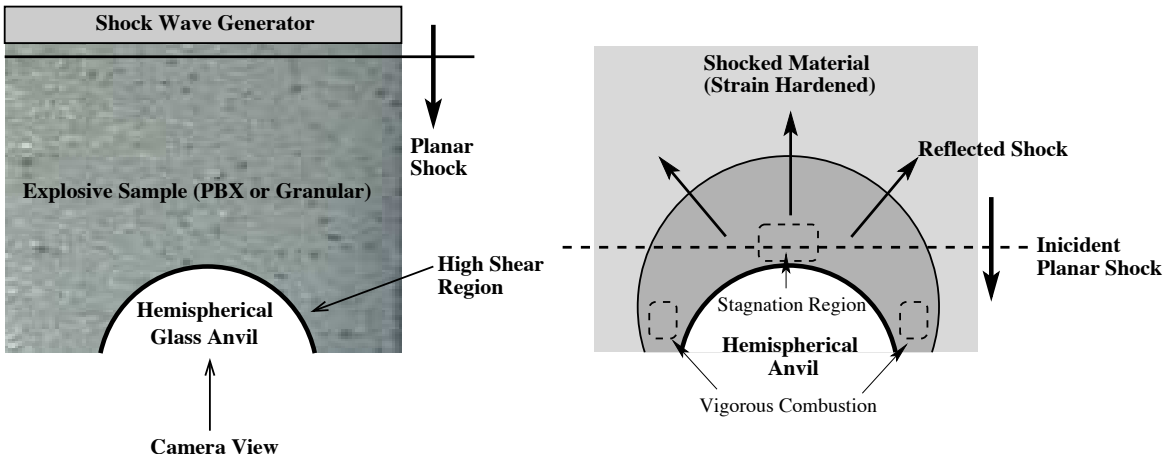

Figure 1: Illustration of the experimental test geometry used to characterize the combined shock-shear behavior of explosives.

initiated vigorous combustion near the explosive-anvil boundary away from the high-pressure stagnation region; an illustration of the test configuration is shown in Fig. 1. This observation suggests that macro-scale shear may be important for combustion initiation, though its precise role remains unclear. Analysis of deformation wave-boundary interactions is warranted because they commonly occur in practice, but such analysis is complicated by the existence of multi-scale processes that arise due to material heterogeneity; the initial distribution of particle sizes may range from 0.001-200 μm, whereas the size of engineered materials is orders of magnitude larger. Also, length and time scales of physical phenomena occurring at the particle and macro-scales may vastly differ; dissipative heating can occur rapidly over length scales that are much smaller than the average particle size, whereas detonation of explosives resulting from low pressure impact can occur slowly over comparatively large distances (≈ 4 cm). Though it is well-accepted that material heterogeneity gives rise to deformation wave structures exhibiting intense particle-scale fluctuations, the relative importance of dissipative mechanisms and their influence on macro-scale behavior remain largely unresolved issues, particularly for problems involving wave-boundary interactions. Consequently, multi-scale computational examination of such interactions is warranted, particularly in the absence of particle-scale data.

In the remaining sections of this report, key objectives of this work, and research methods used, are first summarized, followed by a discussion of key results. A list of research personnel supported by this work, and of publications and presentations which resulted from it, are then given.

2 Objectives and Research Method

Motivated by the experiments of Ref. [11], an overall objective of this study was to computationally examine multi-scale dissipative heating induced by the interaction of initially planar deformation waves in granular explosive with macro-scale boundaries and to characterize its dependence on initial wave strength. To this end, computations were independently performed using both macro-scale and meso-scale model descriptions to obtain a better understanding of this process. The macro-scale description can be applied to engineering scale systems, but does not explicitly resolve particle-scale temperature fluctuations (referred to as hot-spots) that are important for combustion initiation. The meso-scale description resolves particle-scale fluctuations, but cannot be faithfully applied to engineering scale systems due to computational limitations. This work is a preliminary

step towards a longer term goal of using meso-scale computations to facilitate development of improved macro-scale constitutive theories for impact induced phenomena occurring in heterogeneous energetic solids. It is noted that the meso-scale modeling effort, which represents a significant component of the work performed, was not part of the original scope of the proposed project. This supplemental effort was undertaken to provide information about deformation particle-boundary interactions, including particle-scale dissipative heating, in the absence of experiments. Combined shock-shear experiments for granular explosive planned by AFRL-MNME personnel that were to guide development of a macro-scale constitutive theory for this project were suspended due to programmatic issues. The objectives and research method for both the macro-scale and meso-scale modeling and computational efforts are summarized below.

2.1 Macro-Scale Modeling and Computations

Objectives. Specific objectives of the macro-scale modeling and computational effort included the following:

1. *Analysis of Deformation Wave Interactions with Planar Boundaries.* (See Ref. [6] for a comprehensive discussion.) The objective of this study was to computationally examine interaction between an incident planar deformation wave in granular HMX explosive (octahydro-1,3,5,7-tetranitro-1,3,5,7-tetrazocine) and a rigid planar boundary that deflects the flow through an angle θ, as illustrated in Fig. 2(a). Granular HMX was chosen because its uniaxial compaction behavior is reasonably well-characterized [3, 4]. The planar boundary represents a theoretically simpler configuration for assessing deformation wave-boundary interactions than those associated with more complex boundary geometries. Particular emphasis was placed on characterizing how incident deformation wave strength, expressed in terms of a piston impact speed U_p, and flow turning angle θ affect interaction structure and dissipative heating of the explosive, where $0^\circ \leq \theta \leq 90^\circ$. The limiting values $\theta = 0^\circ$ and 90° result in no boundary interaction and pure reflection, respectively. This computational analysis also enabled the effects of rapid, repeated loading to be investigated as material pre-compacted by the incident planar deformation wave was subsequently deformed by reflected waves. As such, a secondary objective of this effort was to examine how rapid, repeated loading of explosive affects its sensitivity; this represents a largely unanswered question that has important ramifications in practice.

2. *Analysis of Deformation Wave Interactions with Non-Planar Boundaries.* (See Refs. [5, 6] for a comprehensive discussion.) The objective of this study was to computationally examine interaction between an incident planar deformation wave in granular HMX and a rigid semicircular boundary. This configuration was chosen to mimic the experimental configuration of Ref. [11], depicted in Fig. 1; the computational domain used in this study is shown in Fig. 2(b). For this configuration, the flow deflection angle decreases with position along the boundary surface. As with the planar boundary study, emphasis was placed on characterizing how deformation wave-boundary interaction structure and explosive dissipative heating varies with incident wave strength.

Research Method. (A comprehensive discussion of the model, numerical technique, and its verification and validation for granular HMX, is given in Refs. [3, 4, 6].) The macro-scale model used in this study is an extension of a continuum field theory for the Deflagration-to-Detonation Transition (DDT) of granular explosive, first formulated by Baer and Nunziato [1], and later improved by

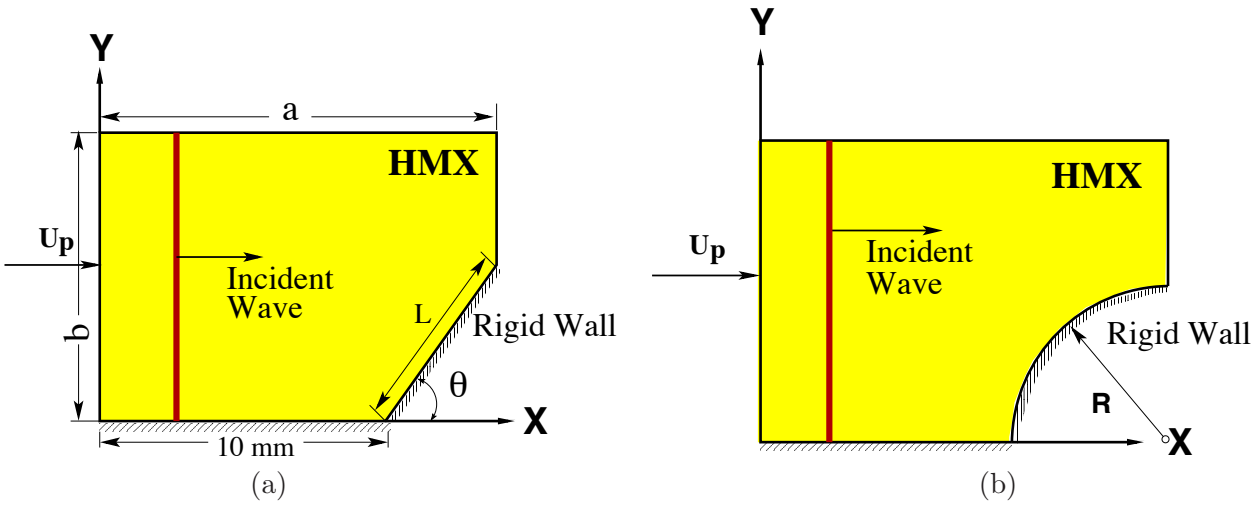

Figure 2: Computational domains used to investigate the interaction of initially planar macro-scale deformation waves in granular explosive with (a) rigid planar boundaries and (b) rigid circular boundaries.

Bdzil, et al [2], to account for both elastic and inelastic volumetric deformation in a thermodynamically consistent manner [3, 4]. For inert impact, $\epsilon \equiv \rho_g/\rho_s \ll 1$, where ρ_g and ρ_s are the gas and solid density; thus, gas phase effects were ignored in this study. In this limit, the evolution of mass, momentum, energy, solid volume fraction, and no-load (inelastic) solid volume fraction were described by:

$$\frac{\partial \mathbf{q}}{\partial t} + \frac{\partial \mathbf{f}}{\partial x} + \frac{\partial \mathbf{g}}{\partial y} = \mathbf{s}, \tag{1}$$

where

$$\mathbf{q} = \left[\rho, \rho\, u, \rho\, v, \rho\, E, \rho\phi, \rho\,\tilde{\phi}\right]^{\mathrm{T}},$$
$$\mathbf{f} = \left[\rho u, \rho u^{\,2} + P, \rho uv, \rho u(E + P/\rho), \rho\phi u, \rho\tilde{\phi} u\right]^{\mathrm{T}},$$
$$\mathbf{g} = \left[\rho v, \rho\, uv, \rho v^{\,2} + P, \rho v(E + P/\rho), \rho\phi v, \rho\tilde{\phi} v\right]^{\mathrm{T}},$$
$$\mathbf{s} = \left[0, 0, 0, 0, \frac{\rho\phi(1-\phi)}{\mu_c}\left(P_s - \beta\right), \rho\Lambda\right]^{\mathrm{T}},$$

and

$$\Lambda = \begin{cases} \frac{1}{\tilde{\mu}}\left(f - \tilde{\phi}\right) & \text{if } f(\phi) > \tilde{\phi}, \\ 0 & \text{otherwise.} \end{cases}$$

In these equations, $\rho = \phi\rho_s$ and $P = \phi P_s$ are the effective density and pressure of the granular solid, where ϕ is the solid volume fraction and P_s is the solid pressure; $E = e_s + B + (u^2 + v^2)/2$ is the mass-specific total energy of the granular solid, where e_s is the solid internal energy and B is the compaction potential energy; $\tilde{\phi}$ is the inelastic component of the solid volume fraction; β is a configurational stress that resists compaction; and f is a yield function that establishes the onset of inelastic volumetric deformation. The parameters μ and $\tilde{\mu}$ establish the rates of stress equilibration and relaxation to the yield surface, respectively.

Of particular importance in this analysis is the heating of solid explosive because of its relevance to combustion. For low pressure waves, the dominant heating mechanism is volumetric deformation

by compaction, where the mass-specific compaction induced dissipative heating rate is given by:

$$\begin{aligned} \dot{w}_c &= \dot{e}_\phi + \dot{e}_{\tilde{\phi}} \\ &= \frac{(P_s - \beta)}{\rho}\frac{d\phi}{dt} + \frac{\beta}{\rho}\frac{d\tilde{\phi}}{dt}. \end{aligned} \tag{2}$$

Here, $d(\bullet)/dt \equiv \partial(\bullet)/\partial t + \mathbf{v}\cdot\nabla(\bullet)$ is the Lagrangian derivative. The first term accounts for rate-dependent dissipation (it vanishes for slow compaction because $P_s \approx \beta$), whereas the second term accounts for dissipation due to inelastic deformation. It is noted that the inclusion of $\tilde{\phi}$ in the theory enables split wave structures to evolve that are analogous to elastic-plastic waves in dynamically loaded homogeneous solids [4].

The governing equations, expressed in terms of generalized curvilinear coordinates, were numerically integrated using a high-resolution, shock-capturing technique. The technique is nominally second-order accurate in space, and third-order accurate in time.

2.2 Meso-Scale Modeling and Computations

Objectives. Specific objectives of the meso-scale modeling and computational effort included the following:

1. *Analysis of Micro-Cluster Impact with a Planar Wall.* (See Refs. [7, 8, 9] for a comprehensive discussion.) The objective of this study was to computationally examine inert, plane strain (2-D), impact of a small, close, randomly packed, and numerically well-resolved micro-particle cluster ($\approx$ 25 particles) with a planar boundary, as illustrated in Fig. 3(a). Emphasis was placed on characterizing the variation in temporal and spatial partitioning of energy within the material with impact angle θ, and on identifying the relative importance of plastic and friction work as potential hot-spot formation mechanisms. These high velocity micro-clusters might originate in practice, for example, from the break-up and dispersal of energetic solids by strong shocks. This analysis is important for the following reasons. First, the impact angle will always vary for loading events in practice. Second, bulk experiments indicate that combustion of energetic solids often first occurs near the impactor surface, implying that particle heating is largest at that location. Third, uncertainty exists about the coupled effects of particle-wall and particle-particle frictional interactions on stress and energy states within dynamically loaded materials and how they can facilitate reactive hot-spot formation. Last, the development of suitable multi-dimensional boundary conditions for use with bulk scale models requires a firm understanding of particle scale physics occurring in the immediate vicinity of solid boundaries. This problem provides a rational foundation for additional study on the influence of far-field particle interactions (i.e., particle self-confinement), phase change, and combustion on the 3-D near wall impact response.

2. *Analysis of Uniaxial Deformation Wave Structure.* (See Refs. [8, 10] for a comprehensive discussion.) The objective of this study was computationally examine meso-scale energy partitioning within uniaxial, quasi-steady deformation waves due to constant speed piston impact; the computational domain is illustrated in Fig. 3(b). Particular emphasis was placed on characterizing the evolution of hot-spot mass fraction within the wave structure and its dependence on impact speed, and to identify the relative importance of plastic and friction work as hot-spot mechanisms. Quasi-1D macro-scale predictions were obtained and analyzed by averaging the meso-scale response over suitable material volumes. A further objective of

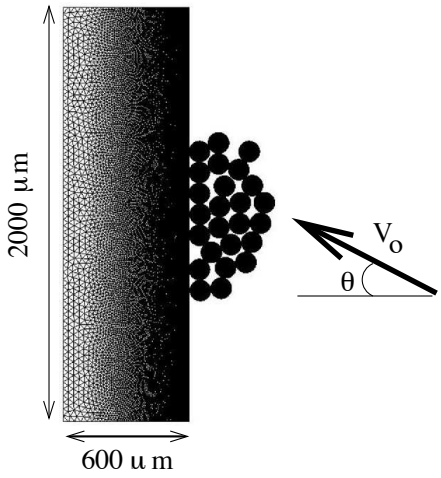

(a)

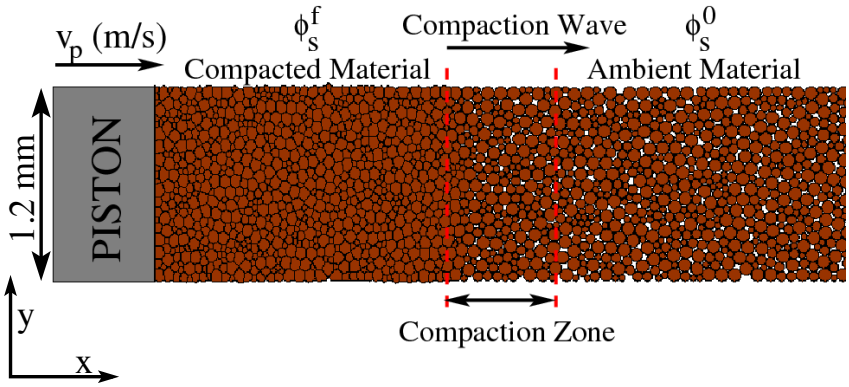

(b)

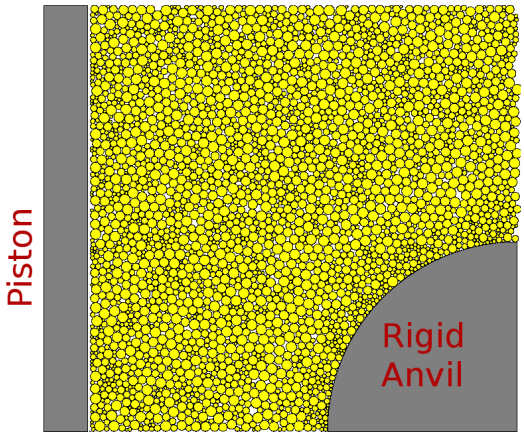

(c)

Figure 3: Computational configurations used for the meso-scale analysis: (a) micro-cluster impact; (b) uniaxial deformation waves; and (c) deformation wave interactions with non-planar boundaries.

this study was to characterize the dependence of deformation wave structure and hot-spot formation on constitutive parameters and material meso-structure. Key constitutive parameters considered included the plastic viscosity, which establishes the time scale for rate-dependent relaxation to the material yield surface, and the friction coefficient, which establishes the magnitude of the surface traction at inter-particle contact surfaces. This study is important because both of these parameters, which are difficult to experimentally determine under impact conditions, can significantly affect the particle and macro-scale mechanics. Also, most energetic materials used in practice have a non-uniform particle size distribution so that high volumetric packing densities can be obtained. It may also be possible to promote a desired effect (e.g., impact sensitivity and combustion rate) by carefully controlling the initial particle size distribution of the material; this possibility requires a reasonable understanding of meso-scale physics. Therefore, simulations were also performed for materials having different initial particle size distributions to demonstrate their effect on both deformation wave structure and hot-spot formation.

3. *Analysis of Deformation Wave Interactions with Non-Planar Boundaries: Comparison with Macro-Scale Predictions.* (See Ref. [5] for a comprehensive discussion.) The objective of this study was to computationally examine the 2-D inert heating response of granular explosive due to interaction of an initially planar compaction wave with a semi-circular rigid anvil; the initial computational domain is illustrated in Fig. 3(c). The meso-scale model combined conservation principles with an elastic-viscoplastic constitutive theory to predict contact induced thermomechanical fields within particles. Meso-scale field predictions were locally averaged and compared to those given by the macro-scale model. Emphasis was placed on characterizing the evolution of spatial wave structure, compaction induced heating rate, and hot-spot mass in the vicinity of the anvil surface, and their dependence on initial wave strength. This analysis is important because the interaction between deformation waves in granular explosive and non-planar macro-scale boundaries, which commonly occur in practice, may locally trigger prompt vigorous combustion due to high dissipative heating rates, as mentioned. A long term objective of this work is to correlate meso-scale hot-spot predictions with macro-scale quantities, such as porosity, pressure, and volumetric deformation rate, for use with a macro-scale combustion theory.

Research Method. (A comprehensive discussion of the numerical modeling technique, and its verification and validation for granular HMX, is given in Refs. [8, 9].) Multi-body contact induced by dynamic compaction was posed as a coupled initial-boundary-value problem (IBVP) for the displacement field $\mathbf{u}$ and temperature field T within particles. These fields were described by momentum and energy evolution equations within each particle:

$$\rho\ddot{\mathbf{u}} = \boldsymbol{\nabla}\cdot\boldsymbol{\sigma}, \tag{3}$$

$$\rho c_v\dot{T} = -\boldsymbol{\nabla}\cdot\mathbf{q} + \rho r. \tag{4}$$

Here, ρ is the local mass density, $\boldsymbol{\sigma}$ is the Cauchy stress tensor, r is the deformation induced heating, $\mathbf{q}$ is the heat flux, c_v is the specific heat at constant volume, and $\boldsymbol{\nabla}\equiv\partial(\cdot)/\partial\mathbf{x}$ is the spatial gradient operator. Body forces were ignored as they are inconsequential compared to impact induced deformation forces. All particles were initially stationary, stress free, and at a uniform ambient temperature. Only contact boundary conditions were imposed on the displacement and temperature fields of the particles:

$$\boldsymbol{\sigma}\cdot\mathbf{n} = \mathbf{t}_c \text{ on}\Gamma \quad \forall\, t, \tag{5}$$

$$(-k_T\boldsymbol{\nabla}T)\cdot\mathbf{n} = q_f + q_c \text{ on}\Gamma \quad \forall\, t, \tag{6}$$

where Γ is the particle boundary, $\mathbf{n}$ is the unit normal to Γ, $\mathbf{t}_c$ is the contact traction, k_T is the thermal conductivity, q_f is the heat flux due to frictional heating, q_c is the heat flux necessary to impose ideal thermal contact, and t is time. The system of equations was closed by prescribing a constitutive theory for the stress response. To this end, a hyperelastic, multiplicative, finite strain constitutive theory was used to model stress-strain behavior. A Perzyna type over-stress model, coupled with an associative flow rule and a Von-Mises type yield criterion with isotropic hardening, was used to prescribe the evolution of inelastic strain. Material properties used in this study were chosen to be representative of the secondary high explosive HMX.

Simulations were performed using a combined finite and discrete element method that is well-suited for problems involving heterogeneity. This combined method used the finite-element method (FEM), coupled with a radial return stress update algorithm, to numerically integrate the time-dependent, 2-D conservation principles and viscoplastic flow rule governing deformation of individual particles, and used the discrete-element method (DEM) to account for interactions between particles. The DEM was based on a distributed, conservative potential based penalty method whereby the normal contact traction between particles was estimated by penalizing their penetration, and frictional tractions were estimated using a penalty regularized Amonton's Coulomb law. Particles were discretized using constant strain, triangular finite elements, where each particle consisted of 400-1200 elements for all simulations performed in this work. A temporally second-order accurate, explicit numerical technique was used to integrate the finite element equations for nodal displacements and temperatures.

3 Key Results

The following summary highlights key results for the objectives identified in Section 2.

3.1 Macro-Scale Modeling and Computations

1. *Analysis of Deformation Wave Interactions with Planar Boundaries.* (See Ref. [6]) The inert impact response of initially planar deformation waves in granular HMX with rigid planar boundaries was computationally examined [Fig. 2(a)]. Emphasis was placed on characterizing how initial wave strength and wave deflection angle θ affect interaction structure and explosive dissipative heating. To this end, the steady 1-D equations [obtained from Eq. 2], valid in a wave-attached frame, were numerically integrated as an Initial-Value-Problem (IVP) to obtain the spatial wave structure corresponding to a specified impact speed U_p; the resulting structure was then interpolated onto the 2-D computational grid. The initial radius of HMX particles was taken to be $r = 100$ μm, and the initial solid volume fraction was taken to be $\phi_0 = 0.85$. Initial wave strengths corresponding to $U_p = 15$, 120 and 300 m/s were investigated because of differences in their spatial structure: the structure for $U_p = 15$ m/s possesses only a viscoelastic region, whereas the structures for $U_p = 120$ and 300 m/s possess a viscoelastic precursor followed by a viscoplastic region (see Ref. [4] for a comprehensive discussion of planar deformation wave structures in granular explosive). The wave deflection angle was varied between $0^\circ \leq \theta \leq 90^\circ$.

   Dispersed wave-boundary interaction structures were predicted that are analogous to those given by gas dynamics for the interaction of shocks with planar boundaries. As illustrated in Fig. 4 for $U_p = 120$ m/s, interaction structures generally consisted of three intersecting waves: an incident wave, a stem wave near the boundary surface (analogous to a Mach stem), and a reflected wave. The relative strengths of these waves depend on U_p and θ. For

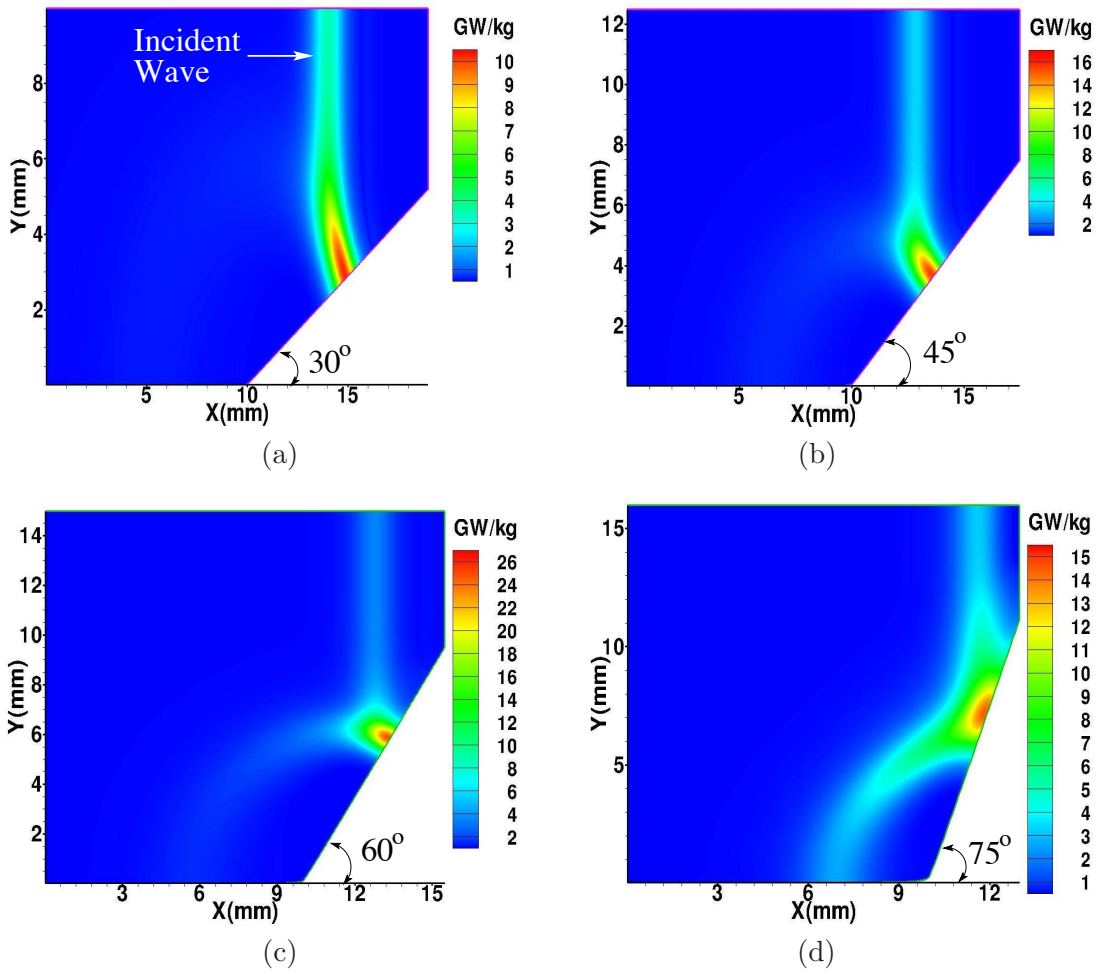

Figure 4: Predicted mass-specific dissipative heating rate contours for the interaction of an initially planar deformation wave with a rigid planar boundary for $U_p = 120$ m/s: (a) $\theta = 30°$, (b) $\theta = 45°$, (c) $\theta = 60°$, and (d) $\theta = 75°$. The spatial contours shown do not necessarily correspond to the time of maximum heating.

values of U_p considered in this study, these waves propagate at subsonic speeds relative to the ambient pure phase explosive, and have finite thicknesses due to deformation induced dissipation (unlike gas dynamic waves). The wave speeds increase, and thicknesses decrease, with increasing U_p. Borrowing terminology from gas dynamics, Von Neumann reflections are predicted for approximately $0° < \theta \leq 30°$, Mach reflections are predicted for approximately $30° < \theta \leq 60°$, and regular reflections are predicted for approximately $\theta > 60°$. Deflection angles which define these different flow regimes are dependent on U_p.

The dissipative heating rate [given by Eq. 2] is particularly important because of its relevance to combustion initiation; it is predicted to increase above that of the incident wave along the surface of the planar boundary due to the interaction process. For a given initial wave strength and material porosity, the peak heating rate is associated with Mach reflections, as illustrated in Fig. 4(c) for $U_p = 120$ m/s and $\theta = 60°$. Peak heating rates of $\dot{w}_c = 6.5$, 13, 25, 40, 16, and 10 GW/kg were predicted for $\theta = 15°$, 30°, 45°, 60°, 75° and 90°, respectively. The peak heating rate is lower for $\theta = 75°$ than for 60° because the stem region has weakened

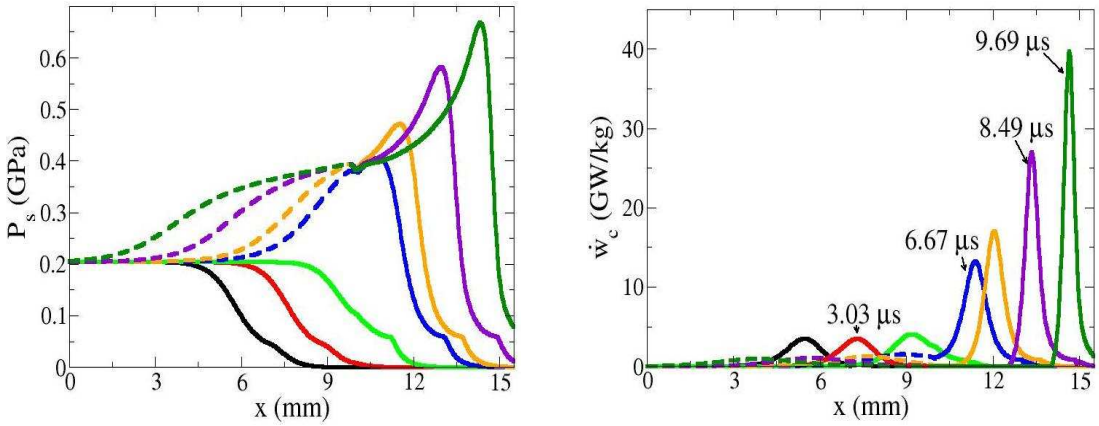

Figure 5: Predicted spatial variation in (a) pressure and (b) mass-specific dissipative heating rate along the lower boundary of the computational domain for $U_p = 120$ m/s and $\theta = 60°$. The tip of the planar boundary is located at $x = 10$ mm. Dash curves denote reflected waves.

as the Mach reflection transitioned to a regular reflection with increasing θ. Importantly, peak heating rates were predicted to occur along the boundary surface near locations of peak pressure for domains investigated in this study, as illustrated in Fig. 5 for $\theta = 60°$. It is also noteworthy that reflected waves generated by wave-boundary interactions, which propagate back through material pre-compacted by the incident wave, induce little additional dissipative heating which is indicative of shock desensitization. Predictions for other piston speeds were qualitatively similar to those shown here, but quantitatively differed in terms of heating rates and wave structure.

Dissipative heating rates due to rate-dependent and inelastic deformation [given by $\dot{e}_\phi$ and $\dot{e}_{\tilde{\phi}}$ in Eq. (2), respectively] were also characterized, which depend on both U_p and θ. For $U_p = 15$ m/s, dissipative heating by the incident wave was solely due to rate-dependent (viscoelastic) deformation. However, Mach reflections were shown to induce additional heating by inelastic deformation along the boundary surface for low strength waves which exceeded that due to rate-dependent deformation for large θ. For $U_p = 120$ and 300 m/s, incident waves induced significant dissipative heating due to rate-dependent deformation, whereas dissipative heating due to both rate-dependent and inelastic deformation were shown to be comparable for large θ. These results indicate that wave-boundary interactions can induce complex macro-scale dissipative phenomena that may separately, or in concert, trigger combustion of energetic solids.

2. *Analysis of Deformation Wave Interactions with Non-Planar Boundaries.* (See Refs. [5, 6].) Simulations were performed to characterize macro-scale dissipative heating induced by interaction of initially planar deformation waves in granular HMX with a rigid circular anvil boundary. The initial radius of HMX particles was $r = 70$ μm, and the initial solid volume fraction was $\phi_0 = 0.835$. The anvil radius was taken to be $R = 4$ mm. As done for the planar boundary analysis, the initial wave structure was established by numerically integrating the appropriate 1-D IVP with U_p specified, and interpolating the result onto the 2-D domain.

   Figure 6 illustrates the predicted spatial variation in macro-scale dissipative heating rate [defined by Eq. (2)] for incident waves corresponding to $U_p = 150$, 300, and 450 m/s. Again,

$U_p = 150$ m/s

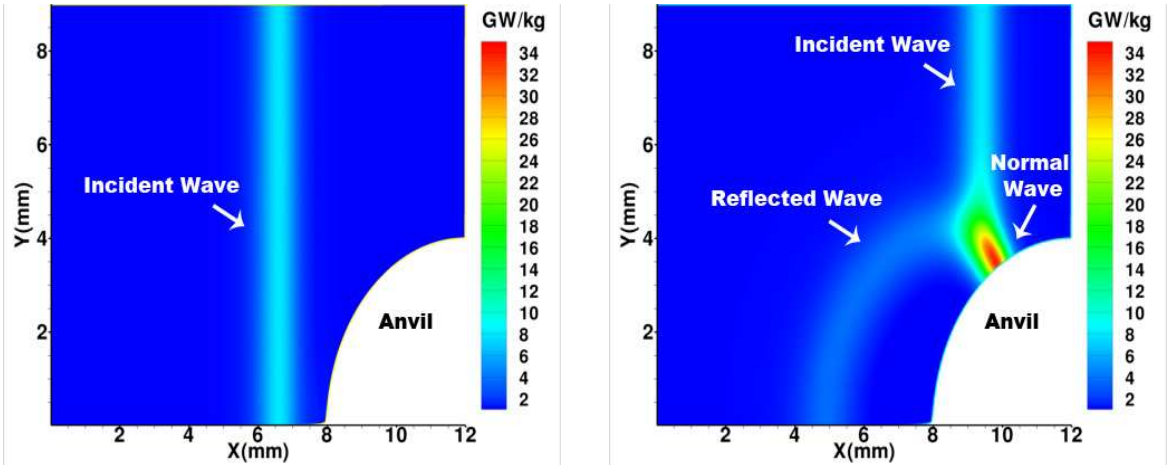

$U_p = 300$ m/s

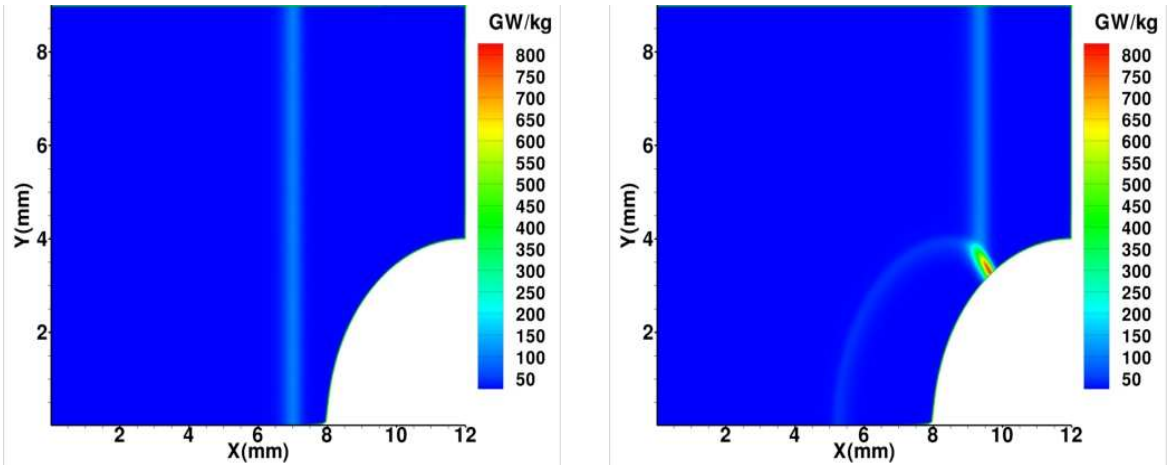

$U_p = 450$ m/s

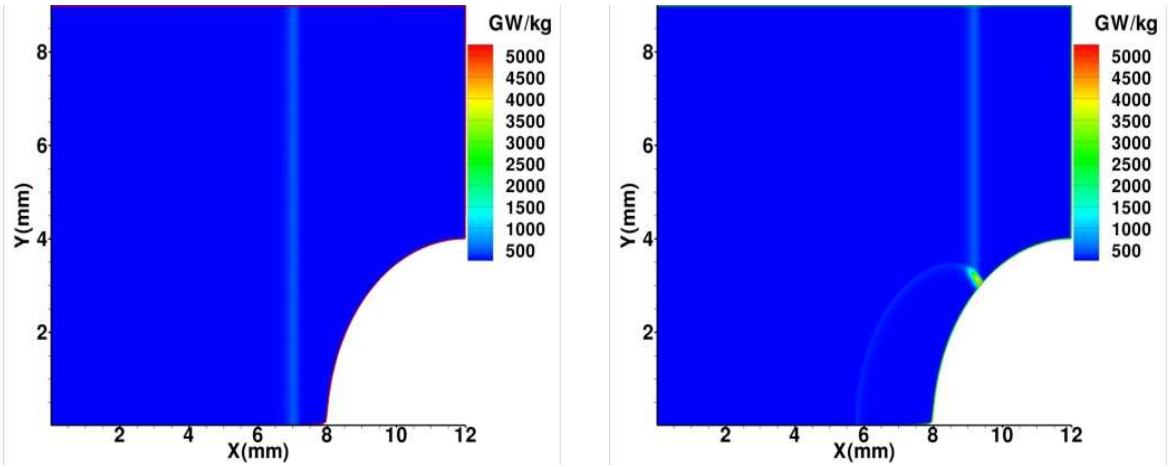

Figure 6: Predicted mass-specific dissipative heating rate contours for the interaction of an initially planar deformation wave with a rigid circular boundary for $U_p = 150$, 300, and 450 m/s. Both early time (left) and late time (right) contours are shown.

interaction structures generally consisted of an incident wave, a stem wave near the boundary surface, and a reflected wave. Dissipative heating rates increased with increasing U_p, with peak heating occurring within the stem region along the boundary surface, whereas wave thicknesses decreased. Shown in Fig. 7 is the predicted spatial variation in heating rate at various times along the bottom of the computational domain for $U_p = 300$ m/s, where the stagnation point of the circular anvil is located at $x = 8$ mm; results were qualitatively similar for all incident wave strengths. Two observations are noteworthy. First, intense heating was induced by the stem wave as it accelerates along the front surface of the anvil and compacts virgin material. A peak heating rate of $\dot{w}_c \approx 800$ GW/kg was predicted to occur at a location along the anvil surface ($x \approx 9.5$ mm) that is removed from the high pressure stagnation region. The peak heating rate was nearly fives times larger than that of the incident wave, and would likely trigger prompt and vigorous combustion of reactive material. The magnitude and location of peak heating rate was dependent on anvil size, but typically occurred near the mid-point of the anvil surface. Second, the reflected wave induced low heating rates because most porosity had already been eliminated by the incident wave, as indicated by the dashed history curves shown in Fig. 7. In this respect, the pre-compacted material had been desensitized to subsequent wave induced deformation. Though not shown here, peak heating rates of $\dot{w}_c \approx 34$ and 5000 GW/kg were predicted for $U_p = 150$ and 450 m/s, respectively.

It should be re-emphasized that dissipative heating induced by wave interactions with planar and circular boundaries qualitatively differed. Peak dissipative heating rates and solid pressures induced by wave interactions with planar boundaries occurred at similar locations along the boundary surface, whereas peak dissipative heating rates induced by interactions with circular boundaries occurred at locations along the boundary surface that were well-removed from the high pressure stagnation region. These predictions are consistent with the experimental observations of Ref. [11] which showed that interaction between an initially planar shock in the explosive PBXW-128 and a hemispherical glass anvil initiated vigorous combustion near the explosive-anvil boundary away from the high-pressure stagnation region, suggesting that maximum heating rate occurred at that location. Moreover, because this analysis ignored the effects of bulk shear, it is likely that combustion initiation may be primarily due to volumetric deformation, with bulk shear being of secondary importance. These predictions collectively indicate that dissipative heating rates induced by wave-boundary interactions are dependent on boundary geometry, and that pressure-dependent models used to describe combustion of energetic solids may provide misleading results for such problems.

3.2 Meso-Scale Modeling and Computations

1. *Analysis of Micro-Cluster Impact with a Planar Wall.* (See Refs. [7, 8, 9].) Impact of an initially stress free, close-packed, 2D micro-particle cluster (25 particles of radii 50 μm) and a planar, rigid wall was computationally examined using a thermoelastic-viscoplastic and stick-slip friction constitutive theory. The influence of impact angle and cluster packing configuration on the spatial and temporal partitioning of dissipated energy was characterized. As illustrated in Fig. 8 for a uniform impact speed 300 m/s, plastic work was shown to rapidly increase near the wall immediately following impact before diffusing outward due to stress transmission between particles, whereas friction work near the wall increased sharply after a very brief initial period of stick (≈ 75 *ns* for normal impact). The initial duration of stick was largest for normal impact and decreased with increase in impact angle. The maximum average plastic work was approximately 4 kJ per unit cluster mass for an impact angle of $\phi = 0^\circ$ (corresponding to normal impact), which was approximately two times larger than that for

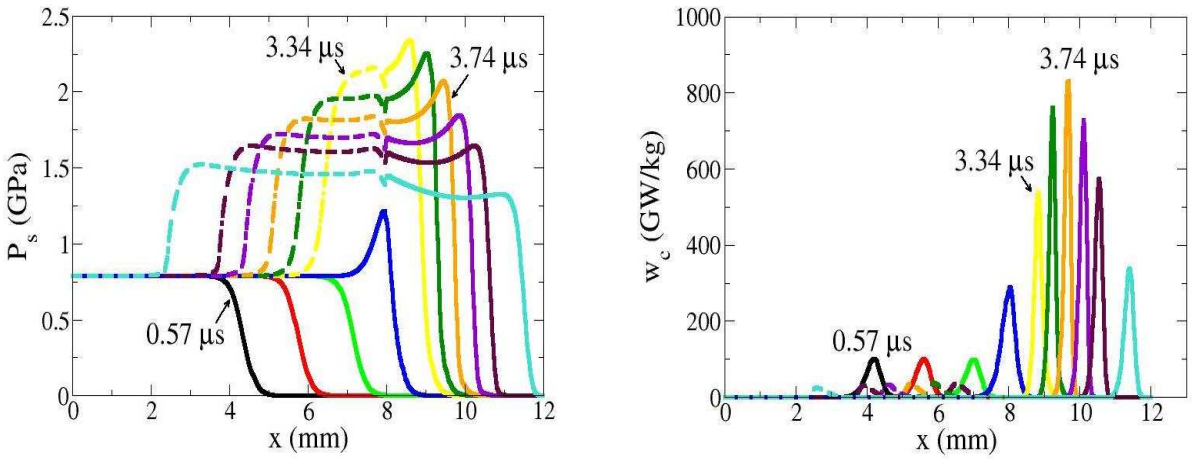

Figure 7: Predicted spatial variation in (a) pressure and (b) mass-specific dissipative heating rate along the lower boundary of the computational domain for $U_p = 300$ m/s. The stagnation point of the circular boundary is located at $x = 8$ mm. Dash curves denote reflected waves.

$\phi = 60°$. The maximum average friction work was approximately 60 kJ per unit cluster mass for $\phi_c = 60°$, which was nine times larger than that for $\phi = 0°$. The critical impact angle for maximum friction work was shown to mildly depend on the initially random cluster configuration, though it is anticipated that little variation in this angle would result for larger particle ensembles. Friction was shown to significantly affect the final cluster kinetic energy, but to minimally affect elastic potential energy and plastic work. Also, particle-wall friction was considerably larger than inter-particle friction due to both the rigid wall assumption and the repeated loading of particles adjacent to the wall by surrounding particles. Predictions from the energy analysis indicated that large temperature rises (≥ 900 K) occur within the cluster, even for normal impact, with the maximum temperature (≈ 4400 K) occurring for $\phi = 80°$. However, the mass heated to such elevated temperatures represented less than .01% of the cluster mass with the most mass ($\approx 98\%$) heated to temperatures rises ≤ 200 K. Localization of dissipated energy indicated that average temperature rises due to friction work exceeded those due to plastic work, even for normal impact, and far exceeded those due to plastic work for highly oblique impact. Average frictionally induced temperature rises near 900 K were predicted for $\phi = 0°$ increasing to 4400 K for $\phi = 80°$. Impact simulations for a deformable wall having thermomechanical properties that are similar to the cluster were only marginally different than the rigid wall results. These predictions collectively highlight the importance of properly describing friction as a local heating mechanism that may induce combustion of energetic particle clusters. This study has provided a foundation for systematically characterizing how other potentially important phenomena, such as wall deformation, particle phase change, and far-field particle interactions, can influence the near wall impact energetics of heterogeneous solids.

2. *Analysis of Uniaxial Deformation Wave Structure.* (See Refs. [8, 10].) Impact induced thermomechanical interactions between deformable particles contained within heterogeneous energetic solids were computationally examined to characterize spatial deformation wave structure, and its dependence on impact speed (v_p = 50-500 m/s), and to identify the relative importance of friction and plastic work as potential hot-spot formation mechanisms. Bulk

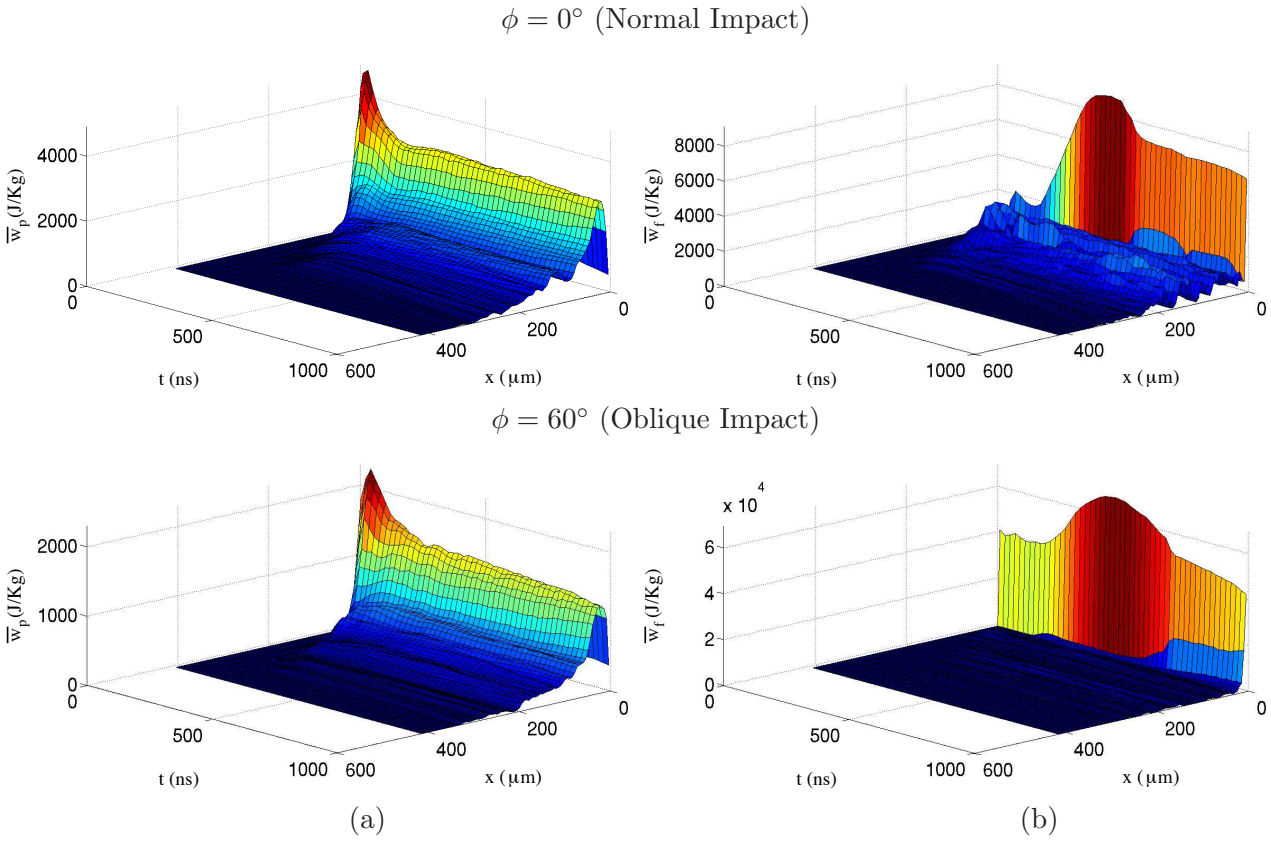

Figure 8: Predictions for the temporal and spatial variation in average specific (a) plastic work and (b) friction work. Here, x is normal distance from the wall.

wave structures having a mostly elastic precursor region, followed by a mostly plastic region in which the porosity is significantly reduced, were predicted for all cases considered in this study, though the lengths of these regions varied with piston speed, as illustrated in Fig. 9. For low piston speeds ($v_p < 100$ m/s), the wave structure was predicted to be thick and dispersed (~ 30 average particle diameters), where compaction was largely due to rigid particle rearrangement rather than plastic void collapse. The particle ensemble was fully compacted for $v_p \geq 400$ m/s due to significant particle plastic deformation associated with void collapse. For these speeds, the wave structure consisted of a very thin precursor zone (~ 1 average particle diameter) followed by a slightly thicker plastic zone (~ 3 average particle diameters). For piston speeds approximately between 100 m/s and 400 m/s, local spatial variations in porosity within the meso-structure, which depend on the initial particle size distribution and packing configuration, induced large amplitude spatial fluctuations in thermomechanical fields behind the wave; the fluctuation magnitudes decreased for higher impact speeds as material strength effects become less consequential. However, it is noted that intra-particle defects (e.g., voids and cracks), which were not modeled in this study, may induce high frequency, large amplitude fluctuations for high impact speeds as the bulk wave thickness decreases.

Plastic work was shown to be the dominant energy dissipation mechanism in that it constitutes a substantial fraction of total system energy (25-35% for $v_p = 50$-500 m/s), whereas friction work constitutes a smaller fraction (2-1% for $v_p = 50$-500 m/s). The maximum plastic and

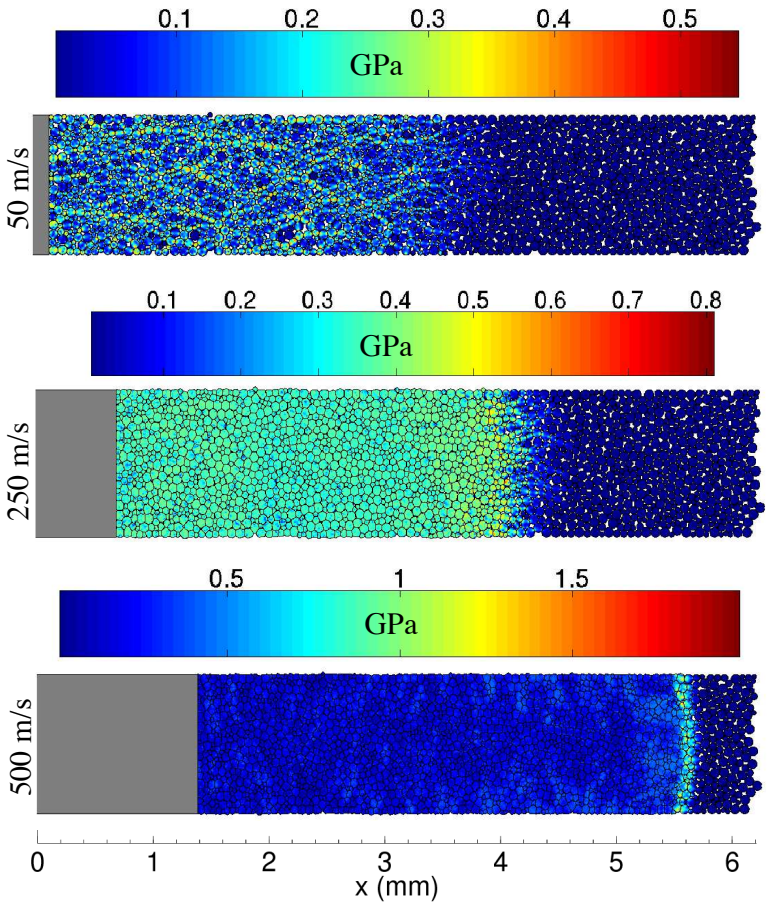

Figure 9: Predicted finite element contours of Von Mises stress $\boldsymbol{\tau}_e$ within particles at 2.75 μ s for $v_p = 50$, 250 and 500 m/s. Values shown in the color-bars are in GPa.

friction work occurred close to the piston boundary due to material and geometry mismatches between the rigid, planar piston and the initially circular particles. Close to the piston, friction work increased from 0.2 J/m to 1.3 J/m for $v_p = 50$ to 500 m/s, whereas plastic work increased from 0.3 J/m to 45 J/m. Predictions for mass-specific friction and plastic work highlighted two important results. First, as illustrated in Fig. 10, mass-specific friction work dominated plastic work for $v_p = 50$ m/s, whereas plastic work dominated friction work for $v_p = 500$ m/s. This result suggests that friction work may be more important than plastic work in producing hot-spots for low pressure impact. Second, friction work is sensitive to details of the meso-structure, particularly for low pressure impact. Predicted maximum hot-spot temperatures far exceeded their average values, even for $v_p = 500$ m/s where a maximum average temperature of only 368 K was predicted; this average value which is well below the approximate ignition threshold for HMX ($T_{ig} \approx 600$ K). Maximum hot-spot temperatures near 600 K were predicted for $v_p = 50\ m/s$, which increased to near 1100 K and 1400 K for $v_p = 250$ m/s and 500 m/s. Meso-scale temperature fields indicated that hot-spots induced by both plastic and friction work are of sub-particle size. Frictionally induced hot-spots occurred along contact interfaces; plastically induced hot-spots occurred within particles in the vicinity of contact surfaces, and they were substantially larger in size and greater in number than frictional hot-spots.

Heated mass was predicted to steadily increase with distance behind the wave front until a quasi-steady value was reached at the end of the compaction zone, with minimal variation with position occurring beyond that location. Minimal heating was predicted within the precursor region of the compaction zone which resulted in temperature rises of$\Delta\ T \leq 5$ K for all cases considered. As illustrated in Fig. 11, quasi-steady, local hot-spot mass fraction distribution curves behind the wave consisted of three parts based on temperature rise intervals$\Delta\ T_b$ and ΔT_f. The first part included mass-fractions ranging from 10^{-1} and 10^{-3} that were heated through a temperature rise of$\Delta\ T_b\ \approx 30$, 100, and 200 K for $v_p = 50$, 250, and 500 m/s. These hot-spots primarily resulted from plastic work occurring within the interior of particles. The second part of the distribution curves included mass-fractions ranging between 10^{-3} to 10^{-4} that were heated through a temperature rise between$\Delta\ T_b$ and$\Delta\ T_f$, where $\Delta T_f\ \approx 70$, 200, and 400 K for $v_p = 50$, 250, and 500 m/s, respectively. These hot-spots resulted from a combination of plastic and friction work occurring in the vicinity of contact surfaces. The third part, or tail, of the distribution curves consisted of small mass-fractions ($m = 10^{-5}$) that experienced$\Delta\ T \geq \Delta T_f$. These hot-spots, which resulted from friction work, varied sporadically with axial position behind the wave due to spatially nonuniform heterogeneities within the meso-structure; they increased in number with piston speed. By comparing hot-spot contours obtained using the predicted temperature field to those estimated using an adiabatic plasticity analysis, where frictional effects and thermal conduction were ignored, revealed that only highly isolated mass (mass-fraction $\sim 10^{-5}$) experienced $\Delta T \geq 25$ K due to plasticity for $v_p = 50$ m/s. For this speed, almost all mass heated above 25 K was entirely due to frictional dissipation. For $v_p = 250$ m/s and 500 m/s, almost all mass heated to $\Delta T \geq 300$ K was due to a combination of plasticity and friction, or friction alone. These predictions collectively highlight that friction work is the more important hot-spot mechanism for low speed impact, and though often ignored, is also significant for high speed impact.

Sensitivity studies were performed to examine the influence of friction coefficient, μ, on compaction wave structure by varying its value from zero to the baseline value of 0.25. Predictions showed that the average porosity behind waves marginally decreased with decreasing friction coefficient due to enhanced particle mobility. Increasing the friction coefficient promoted stick behavior between particles resulting in a more frictionally rigid ensemble. Frictional stick decreased particle mobility at higher friction coefficients which promoted more efficient

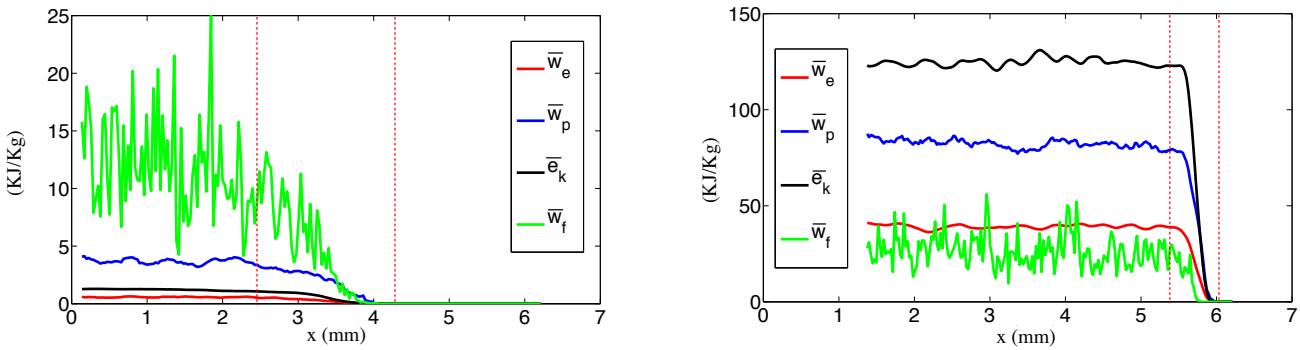

Figure 10: Predictions for the partitioning of average mass-specific system energy at 2.75 μ s for (a) $v_p = 50$ m/s and (b) $v_p = 500$ m/s. In these plots, average mass-specific plastic work is given by $\bar{w}_p$, and average mass-specific friction work is given by $\bar{w}_f$.

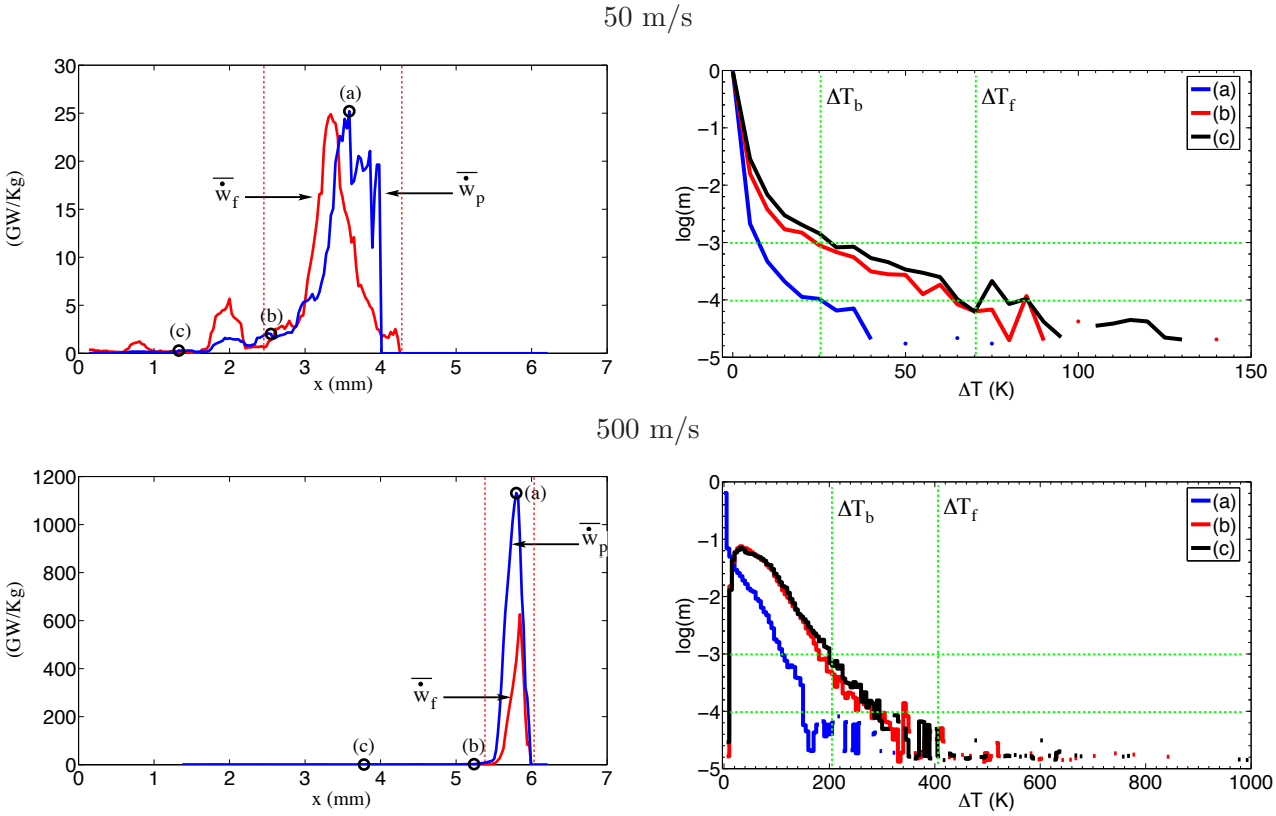

Figure 11: Predicted spatial variation of hot-spot mass-fraction through the compaction wave at 2.75 μ s for $v_p = 50$ and 500 m/s. Plots to the left give the average rates of plastic and friction work. The plots to the right give hot-spot mass fraction at locations indicated in the corresponding plots to the left.

stress transmission between particles and faster bulk wave speeds. Predicted pressure and stress fields showed minimal sensitivity to changes in friction coefficient. Though average temperatures were predicted to marginally increase with friction coefficient, maximum hot-spot temperatures were shown to increase substantially. Peak temperatures of 360, 460 and 660 K were predicted for frictionless cases corresponding to $v_p = 50$, 250 and 500 m/s, respectively, whereas temperatures close to 600, 1100 and 1400 K were predicted for cases have a baseline value of $\mu = 0.25$. Predictions also showed that frictionally induced hot-spot mass-fractions, which constitute the high temperature end of distributions, increased significantly with an increase in friction coefficient, as illustrated in Fig. 12 for $v_p = 250$ m/s.

Sensitivity studies were also performed to examine the influence of plastic viscosity, γ, on compaction wave structure by varying its value from 10 Pa·s to its baseline value of 100 Pa·s. Lowering viscosity increased inelastic deformation rates and resulted in lower porosity behind waves and marginally lower wave speeds. Predicted pressure fields were shown to be insensitive to changes in viscosity. Lower viscosity also resulted in lower average Von Mises stresses $\bar{\boldsymbol{\tau}}_e$ but higher plastic strains $\bar{\epsilon}_p$. Thus, plastic work, given by the product of $\bar{\boldsymbol{\tau}}_e$ and $\bar{\epsilon}_p$, was only marginally affected by the viscosity. Predicted average temperatures were insensitive to viscosity, though peak temperatures increased with viscosity for $v_p > 100$ m/s. Predictions showed that viscosity can substantially enhance the formation of frictionally induced hot-spots, as illustrated in Fig. 13.

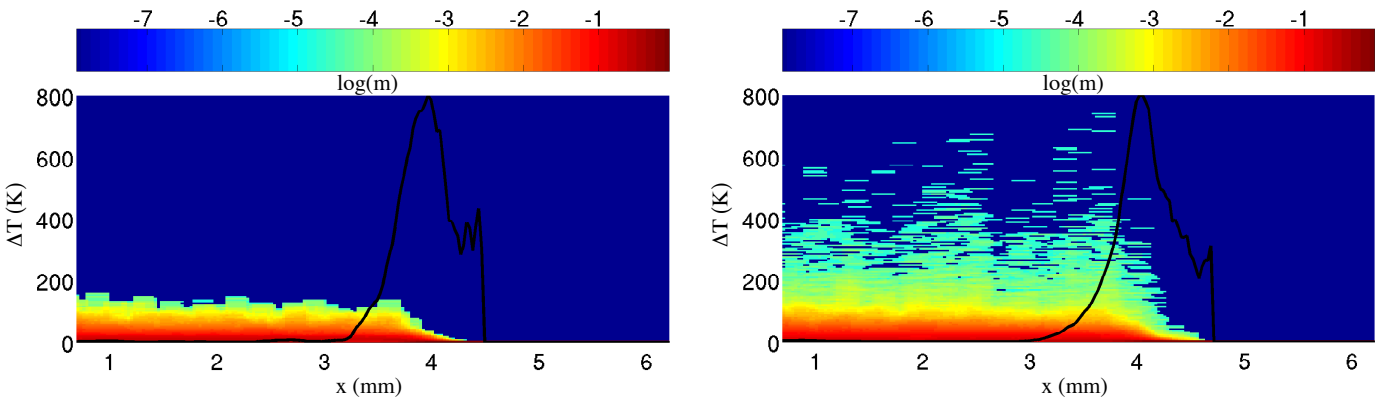

Figure 12: Predicted hot-spot mass-fraction contours for $v_p = 250$ m/s at 2.75 μ s for (a) $\mu = 0.0$ and (b) $\mu = 0.25$. Values in the color-bar represent the logarithm of mass-fraction. The superposed black curves represent the predicted spatial profile for the average rate of plastic work.

Finally, sensitivity studies were performed to examine the influence of initial particle size distribution (PSD) on deformation wave structure. To this end, an alternate particle ensemble was generated that had the same initial porosity as the baseline ensemble, but a wider PSD. Predictions for the mechanical response of both ensembles showed similar qualitative and quantitative trends. The wider PSD resulted in marginally lower porosity behind waves, and wave speeds, due to increased mobility of smaller particles. For a given impact speed, quasi-steady wave pressures for both ensembles were similar, but the stresses within smaller particles exhibited larger spatial fluctuations than those within larger particles. The inelastic deformation and average temperature responses of both ensembles slightly differed, with smaller particles exhibiting higher average temperatures than larger particles. The frictional response was shown to be highly sensitive to PSD in that a wider PSD enhanced frictional dissipation resulting in higher heating rates and temperatures for all piston speeds, as illustrated in Fig. 14. Though smaller particles experienced higher average temperatures, predicted hot-spot mass fraction distributions for each particle size class indicated that larger particles experienced localized heating which more significantly contributed to the high temperature end of the distributions. These predictions suggests that larger particles may play a prominent role in combustion initiation of energetic solids whereas smaller particles may be important for reaction propagation.

3. *Analysis of Deformation Wave Interactions with Non-Planar Boundaries: Comparison with Macro-Scale Predictions.* (See Ref. [5].) Simulations were performed to computationally examine multi-scale interaction of initially planar deformation waves in granular HMX with a semi-circular rigid anvil. The analysis focused on low pressure waves resulting from 100-450 m/s impact. The initial solid volume fraction of the material was taken to be $\phi_0 = 0.835$, and the average grain size was $r_0 = 70$ μm. The anvil radius was taken to be $R = 4$ mm. The domain size was largely chosen based on computational time constraints, and to maintain consistency with the macro-scale analysis; a typical simulation required three days on a parallel computer architecture.

   Figure 15 gives the average mass-specific dissipative heating rate predicted by the meso-scale model for $U_p = 150$, 300, and 450 m/s. Meso-scale averages were locally computed over

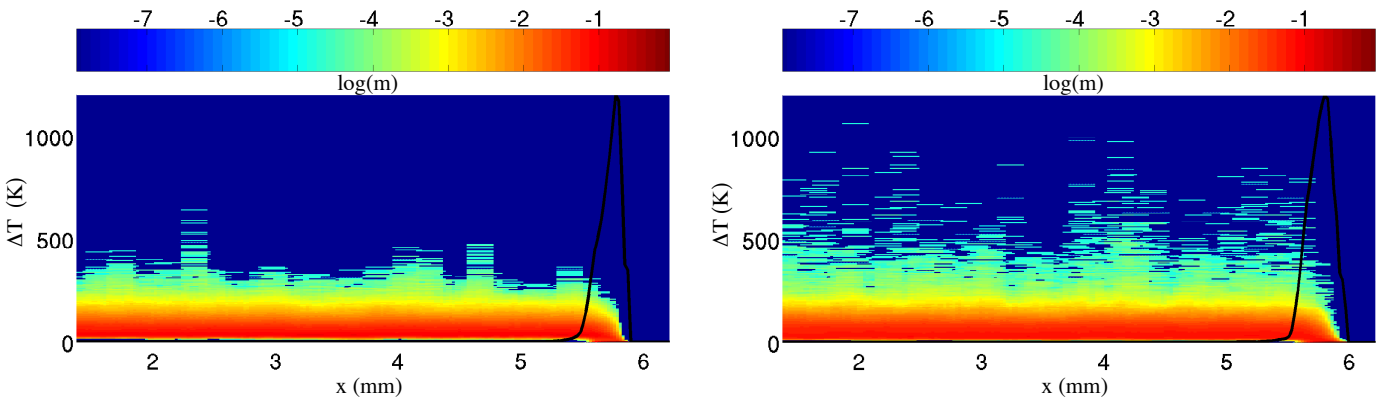

Figure 13: Predicted hot-spot mass-fraction contours for $v_p = 500$ m/s at 2.75 μ s for (a) $\gamma = 1\times10^1$ Pa·s and (b) $\gamma = 1 \times 10^2$ Pa·s. Values in the color-bar represent the logarithm of mass-fraction. The superposed black curves represent the predicted spatial profile for the average rate of plastic work.

a square averaging area of 500×500 μm^2 to facilitate comparison to macro-scale model predictions. Here, the dissipative heating rate was due to viscoplastic deformation of grains during pore-collapse. For all values of U_p, average meso-scale predictions qualitatively agree with macro-scale predictions in that peak heating rates are induced by the stem wave at a location removed from the stagnation region. Also, pre-compacted material was desensitized by the incident wave. However, for approximately $U_p \geq 300$ m/s, the magnitude of heating rates predicted by the meso-scale model were significantly lower than those of the macro-scale model, and wave thicknesses were larger. For these cases, the averaging area width exceeded the wave width causing the average dissipative heating rate within the wave to be unresolved at the macro-scale. For approximately $U_p < 200$ m/s, meso- and macro-scale predictions agreed well both qualitatively and quantitatively based on the averaging area used in this analysis. Establishing the proper choice of averaging area size, and its dependence on material meso-structure and loading conditions, is an important topic of ongoing research.

Meso-scale simulations also provided detailed information about local fluctuations in thermo-mechanical fields that are important for combustion initiation. Of particular importance was the evolution of hot-spot mass fraction distribution. Figure 16 gives predicted distributions for averaging areas located within the stagnation and maximum heating regions. Here, m is the mass fraction and$\Delta\ T \equiv T - T_0$, where T_0 is the ambient temperature. Though the low temperature end of the distributions ($\Delta T \leq 200$ K) were similar in the stagnation and maximum heating rate regions, the high temperature ends departed indicating a substantial increase in hot-spot mass within the latter region. This difference in hot-spot mass is significant, and will likely affect the explosive combustion response. These predictions are again consistent with the experimental observations of Ref. [11]. The coupled dissipative heating-combustion response of the explosive material is an ongoing topic of our research.

4 Personnel Supported

The following personnel were supported during the funding period:

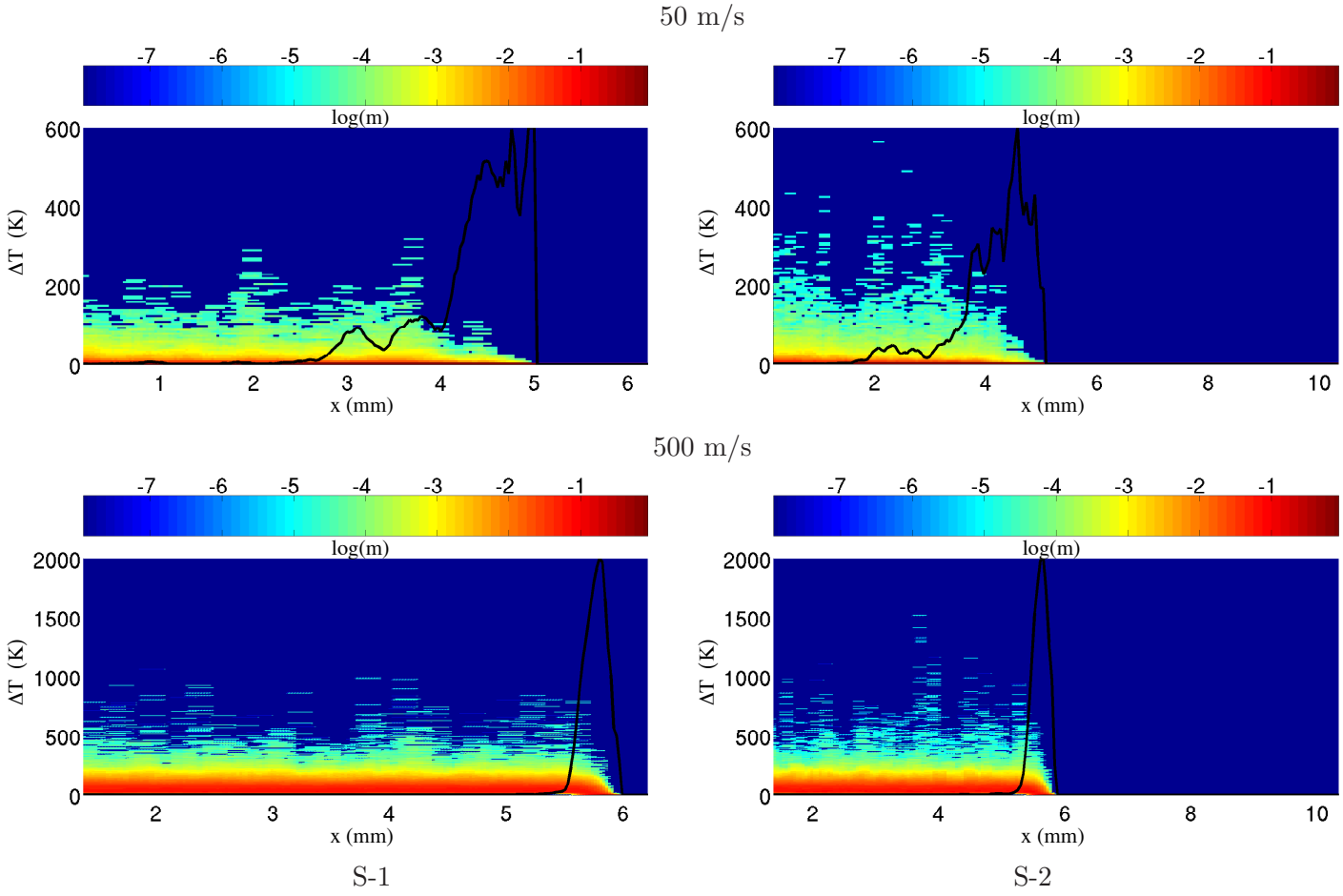

Figure 14: Predicted hot-spot mass-fraction contours for $v_p = 50$ and 500 m/s at 2.75 μ s for configuration S-1 and S-2. Values in the color-bar represent the logarithm of mass-fraction. Configuration S-1 represents the baseline ensemble, and configuration S-2 represents the alternate ensemble having a wider PSD.

- Keith A. Gonthier, Mechanical Engineering Department, Louisiana State University (Associate Professor and PI).
- Rohan Panchadhar, Mechanical Engineering Department, Louisiana State University (Graduate Research Assistant). Ph.D. Dissertation Title: Meso-Scale Heating Predictions for Weak Impact of Granular Energetic Solids, **Completed**–August 2009.
  (Dissertation available at *http://etd.lsu.edu/docs/available/etd-07032009-131245*)
- Anirban Mandal, Mechanical Engineering Department, Louisiana State University (Graduate Research Assistant). M.S. Thesis Title: Computational Analysis of Deformation Wave-Boundary Interactions for Granular Explosive (Anticipated Completion Date–December 2009).

5 Publications and Presentations

Journal publications that resulted from the funded work include the following:

$U_p = 150$ m/s

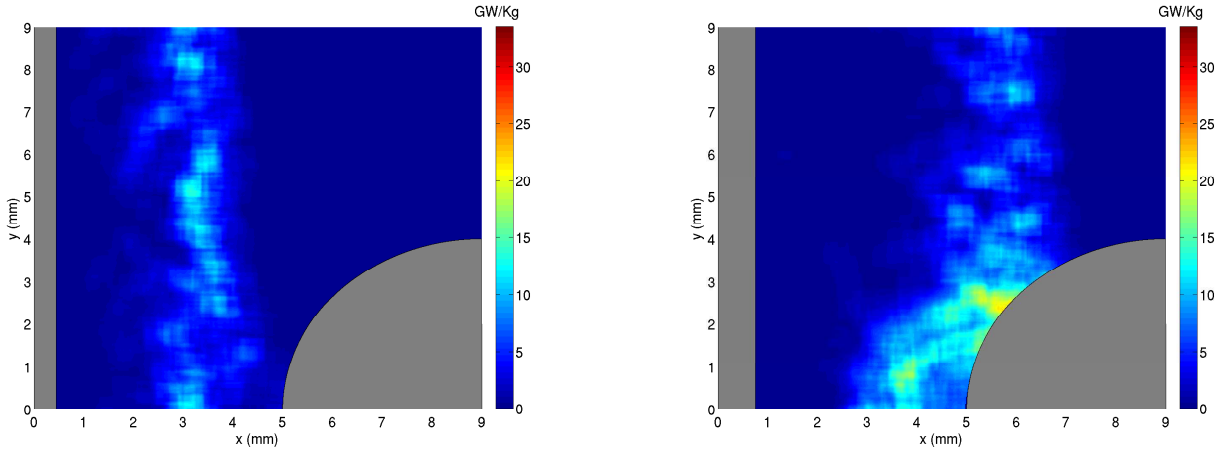

$U_p = 300$ m/s

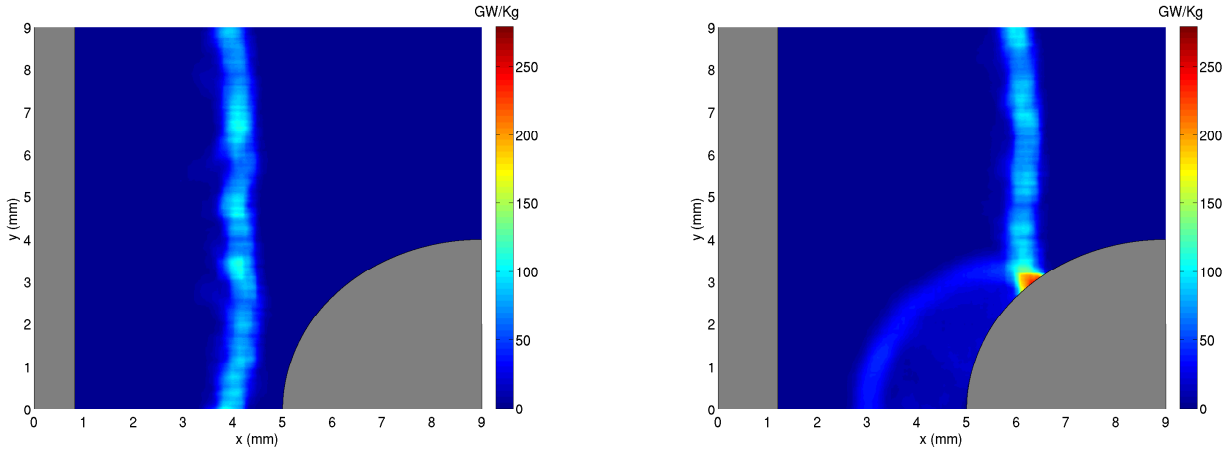

$U_p = 450$ m/s

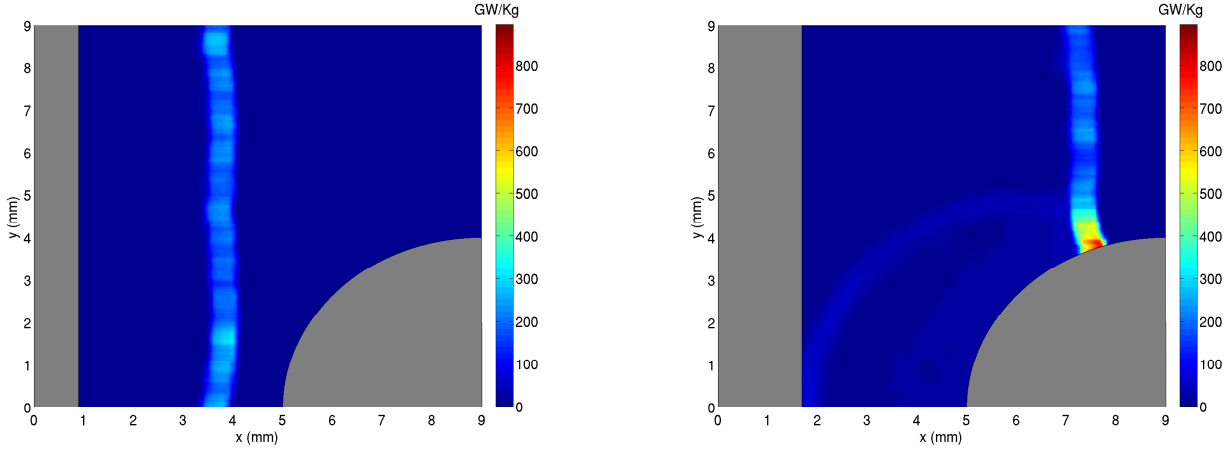

Figure 15: Meso-scale predictions for the average inelastic heating rate induced by the interaction of an initially planar deformation wave and a semi-circular macro-scale boundary.

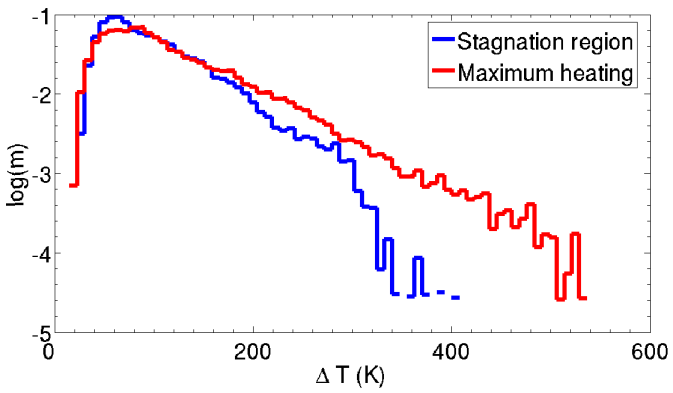

Figure 16: Predicted hot spot mass fraction distribution in the stagnation and maximum heating regions near the anvil surface for $U_p = 450$ m/s.

- Panchadhar, R., and Gonthier, K. A., 2008, "Analysis of Energy Localization Due to Impact Between a Micro-Particle Cluster and a Deformable Wall," *Computer Aided Civil and Infrastructure Engineering*, 23, 265-280.

- Panchadhar, R., and Gonthier, K. A., 2009, "Energy Partitioning within a Micro-Particle Cluster Due to Impact with a Rigid Planar Wall," *Computational Mechanics*, 44(5), 717-744.

Journal publications currently being prepared for submission include the following:

- Mandal, A., Panchadhar, R., and Gonthier, K. A., 2009, "Meso- and Macro-Scale Modeling of Compaction Wave Interactions with a Semi-Circular Macro-Scale Boundary," *Computational Mechanics* (in preparation).

- Panchadhar, R., and Gonthier, K. A., 2009, "Computational Analysis of Plastic and Friction Work Induced by Uniaxial Deformation Waves in Granular Explosive," *Journal of Applied Physics* (in preparation).

- Panchadhar, R., and Gonthier, K. A., 2009, "Effects of Viscoplasticy, Friction, and Material Meso-Structure on Dissipative Heating within Granular Explosive, ," *Journal of Applied Physics* (in preparation).

Conference publications and presentations, that resulted from the funded work include the following:

- Panchadhar, R., and Gonthier, K. A., 2006, "Elastic-Plastic Impact Between a Metal Particle Cluster and a Wall," presented at the 23rd Southeastern Conference on Theoretical and Applied Mechanics (SECTAM XXIII), May 21-23, 2006, Mayaguez, Puerto Rico.

- Gonthier, K. A., 2006, "Deformation Induced Heating and Combustion of Energetic Solids," Decision Applications Division (D-7), Los Alamos National Laboratory, August 15, Los Alamos, New Mexico.

- Panchadhar, R., and Gonthier, K. A., 2007, "Micromechanics of Uniaxial Deformation Waves in Particulate Solids," presented at the ASME Mechanics and Materials Conference, June 3-7, 2007, Austin, Texas.

- Gonthier, K. A., 2008, "Modeling Deformation Waves in Granular Energetic Solids," Particle Mechanics in Extreme Environments Workshop, January 29-31, University of Florida Research and Engineering Education Facility (REEF), Shalimar, Florida.
- Panchadhar, R., and Gonthier, K. A., 2008, "Micromechanics of Quasi-1D Compaction Waves," presented at the 2008 SIAM Annual Meeting, June 7-11, San Diego, California.
- Gonthier, K. A., 2008, "Deformation Waves in Energetic Solids," Joint LSU IGERT-LANL Multiscale CFD Research Symposium, February 28-29, Louisiana State University, Baton Rouge, Louisiana.
- Gonthier, K. A., 2008, "Modeling the Impact Energetics of Particulate Explosives–*Sensitivity*," Air Force Research Laboratory (MNME), August 12, Eglin AFB, Florida.
- Mandal, A., Panchadhar, R., and Gonthier, K. A., 2009, "Computational Analysis of Compaction Wave Interactions with Non-Planar Boundaries," In: *Shock Compression of Condensed Matter*, American Institute of Physics (to appear). Presented at the 2009 APS Topical Conference on the Shock Compression of Condensed Matter (SCCM), June 29-July 3, Nashville, Tennessee.
- Panchadhar, R., and Gonthier, K. A., 2009, "Meso-Scale Heating Predictions for Weak Impact of Granular Energetic Solids," In: *Shock Compression of Condensed Matter*, American Institute of Physics (to appear). Presented at the 2009 APS Topical Conference on the Shock Compression of Condensed Matter (SCCM), June 29-July 3, Nashville, Tennessee.

References

[1] Baer, M. R., and Nunziato, J. W., 1986, "A Two-Phase Mixture Theory for the Deflagration-to-Detonation Transition in Reactive Granular Materials," International Journal of Multiphase Flow, 12, 861-889.

[2] Bdzil, J. B., Menikoff, R., Son, S. F., Kapila, A. K., and Stewart, D. S., 1999, "Two-Phase Modeling of Deflagration-to-Detonation Transition in Granular Materials: A Critical Examination of Modeling Issues," *Physics of Fluids*, 11(2), 378.

[3] Gonthier, K. A., 2003, "Modeling and Analysis of Reactive Compaction for Granular Energetic Solids," *Combustion Science and Technology*, 175, 1679.

[4] Gonthier, K. A., 2004, "Predictions for Weak Mechanical Ignition of Strain Hardened Granular Explosive," *Journal of Applied Physics*, 95(7), 3482.

[5] Mandal, A., Panchadhar, R., and Gonthier, K. A., 2009, "Computational Analysis of Compaction Wave Interactions with Non-Planar Boundaries," In: *Shock Compression of Condensed Matter*, American Institute of Physics (to appear). Presented at the 2009 APS Topical Conference on the Shock Compression of Condensed Matter (SCCM), June 29-July 3, Nashville, Tennessee.

[6] Mandal, A., 2009, Computational Analysis of Deformation Wave-Boundary Interactions for Granular Explosive, MS Thesis, Louisiana State University, Baton Rouge, Louisiana (in progress).

[7] Panchadhar, R., and Gonthier, K. A., 2008, "Analysis of Energy Localization Due to Impact Between a Micro-Particle Cluster and a Deformable Wall," *Computer Aided Civil and Infrastructure Engineering*, 23, 265-280.

[8] Panchadhar, R., 2009, Meso-Scale Heating Predictions for Weak Impact of Granular Energetic Solids, PhD Dissertation, Louisiana State University, Baton Rouge, Louisiana.

[9] Panchadhar, R., and Gonthier, K. A., 2009, "Energy Partitioning within a Micro-Particle Cluster Due to Impact with a Rigid Planar Wall," *Computational Mechanics*, 44(5), 717-744.

[10] Panchadhar, R., and Gonthier, K. A., 2009, "Meso-Scale Heating Predictions for Weak Impact of Granular Energetic Solids," In: *Shock Compression of Condensed Matter*, American Institute of Physics (to appear). Presented at the 2009 APS Topical Conference on the Shock Compression of Condensed Matter (SCCM), June 29-July 3, Nashville, Tennessee.

[11] Wilson, W. H., Tasker, D. G., Dick, R. D., and Lee, R. J., 1998, "Initiation of Explosives Under High Deformation Loading Conditions," Proceedings of the 11th Detonation (International) Symposium, Snowmass, Colorado, pp. 565-572.